Chaos in dynamics: The non-linear waterwheel

Abraham RomeroHernandez

Chaos in Dynamics: The Non-Linear Waterwheel

A Thesis

Presented to the

Faculty of

California State University,

San Bernardino

In Partial Fulfillment

of the Requirements for the Degree

Master of Arts

in

Mathematics

---

by

Abraham RomeroHernandez

September 2012

Chaos in Dynamics: The Non-Linear Waterwheel

A Thesis

Presented to the

Faculty of

California State University,

San Bernardino

by

Abraham RomeroHernandez

September 2012

Approved by:

[redacted]

Dr. Chetan Prakash, Committee Chair

08/16/2012

Date

[redacted]

Dr. Corey Dunn, Committee Member

[redacted]

Dr. Rolland Trapp, Committee Member

[redacted]

Dr. Peter Williams, Chair,
Department of Mathematics

[redacted]

Dr. Charles Stanton
Graduate Coordinator,
Department of Mathematics

ABSTRACT

Chaos in itself has been an intriguing area of study for many mathematicians, physicists, engineers and other scientists. It arises in deterministic systems and is defined as aperiodic behavior that depends sensitively on the initial conditions [Str94]. Chaotic behavior does not occur in linear systems, however it can arise in non-linear systems.

Dynamics is the subject that deals with how systems evolve in time. For any positive integer n and real-valued variables, $x_1, \ldots, x_n$, a dynamical system is the collection of equations

$$\begin{gathered} \dot{x}_1 = f_1(x_1, \ldots, x_n) \\ \vdots \\ \dot{x}_n = f_n(x_1, \ldots, x_n) \end{gathered}$$

where the right-hand side are smooth functions of the variables.

In this thesis basic principles of Chaos in Dynamics will be presented, in the context of the Lorenz Equations [Lor63] :

$$\begin{aligned} \dot{x} &= \sigma(y - x) \\ \dot{y} &= rx - y - xz \\ \dot{z} &= xy - bz. \end{aligned}$$

In particular, we will see a demonstration of chaotic behavior in the Waterwheel Experiment and show how the dynamics of that experiment are a version of the Lorenz equations.

ACKNOWLEDGEMENTS

My research into this field of Mathematics was not an easy one, I did struggle a lot with it and I would not have been able to do it without the people I am going to mention in this acknowledgement. I would like to thank God for everything she has done for me. Special thanks to my main advisor Dr. Chetan Prakash who was willing to take on this subject with me and for all his patience and motivation. My two subadvisors, Dr. Corey Dunn and Dr. Rolland Trapp, and from the Physics Department at CSUSB, Dr. Paul Dixon and Dr. Timothy Usher, for always having your door open to me when I needed adviced or help with my thesis. My parents and siblings, whom I love very much, Concepcion Teresita, Mariano Romero, Hiram, Mariana, and Francisca Romero-Hernandez for all their love, support, struggles, and food. I would like to give special thanks to Kelsi Lynn Miller and M.Ed/M.S. Mathematics Kimberly Grace Raylene Puen for all your support through this thesis and pushing me forward. Thank you Santiago Mondragon Martinez and Armando Martinez for all your help in my thesis and the home-made waterwheel and ideas on how to construct it. Finally, I would like to thank all my friends I have not mentioned; you all have helped me in ways you cannot imagine.

Table of Contents

List of Figures

Chapter 1

Introduction

1.1 Fixed Points and Stability in One-Dimensional Dynamics

In mathematics we describe dynamical behavior as a *system of autonomous ordinary differential equations* in the time-dependent variables $x_1, \ldots, x_n$:

$$\begin{aligned}\dot{x}_1 &= f_1(x_1, \ldots, x_n)\\ &\vdots\\ \dot{x}_n &= f_n(x_1, \ldots, x_n),\end{aligned}$$

where $\dot{x}_j \equiv \dfrac{dx_j}{dt}$, for $j = 0, 1, \ldots, n$ [Str94]. Here t is time and the system is called autonomous because there is no explicit time dependence in the right-hand sides. To determine the behavior of such dynamic systems, it is best to find their *phase portraits*, i.e., the trajectory of the vector $\mathbf{x} = (x_1, \ldots, x_n)$ through any given initial vector. If $f_1, \ldots, f_n$ are sufficiently smooth, such trajectories exist and are unique. It is usually impossible to find such trajectories in closed-form solution, so the best we can do is often to make a more qualitative study of the phase space. For this purpose, it is useful to explore the stability properties in phase space. In particular, we look for equilibrium points or cycles to see how solutions should behave near them. We will first look at equilibria, or fixed points.

Fixed points, also called *nodes*, of a system are any vectors $(x_1, \ldots, x_n)$ for which $\dot{x}_i = 0$ for all $i = 1, \ldots, n$. For this thesis, the fixed points of the system will be denoted by $\mathbf{x}^*$. Take for example $\dot{x} = 1 - x^2$. Setting $\dot{x} = 0$, it is determined that its fixed points are $\mathbf{x}^* = \mp 1$; since that is when $\dot{x} = 0$. This can be clearly seen by the graph of $f(x)$ in Figure 1.1

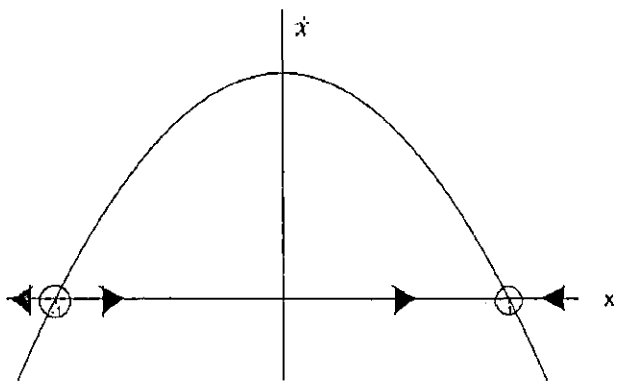

Figure 1.1: $f(x) = 1 - x^2$ Graph

Figure 1.1 is called a *phase portrait*. Phase portraits show the *trajectories* of the dynamics systems. In this case, the phase portrait of Figure 1.1 shows the trajectories for $\dot{x} = f(x) = 1 - x^2$, along the x-axis. The graph of $f(x)$ not only allows us to see the behavior of the trajectories of a system, but it also tells us the stability of the fixed points. Fixed points can either be unstable, stable, or half-stable, which we symbolize as in Figure 1.2

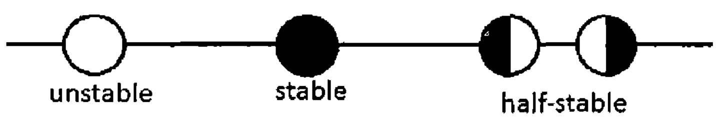

Figure 1.2: Stability of Fixed Points

To determine the stability of the fixed points, we must first find the flow of the trajectory on the pase portrait. If $f(x) < 0$, $\dot{x} < 0$ and x is decreasing, so the flow is to the left, denoted by a left arrow; and if $f(x) > 0$, $\dot{\mathbf{x}} > 0$ is increasing, then its flow is to the right, denoted by a right arrow on the phase portrait [Str94]. Lets look at the phase portrait, Figure 1.1, of the previous example $\dot{x} = 1 - x^2$. We can see that the flow of $f(x)$ is to the left for when $x < -1$ since $f(x) < 0$. When $-1 < x < 1$, $f(x) > 0$ so the flow is to the right. Finally the flow is to the left for $f(x) < 0$ when $\mathbf{x}^* > 1$. Hence, at $\mathbf{x}^* = -1$ the fixed point is unstable since the flows on the left and right are going away from this fixed point. The fixed point $\mathbf{x}^* = 1$ is stable since the flow on the right and left of it are pointing towards it. So, combining Figures 1.1 and 1.2, we have Figure 1.3.

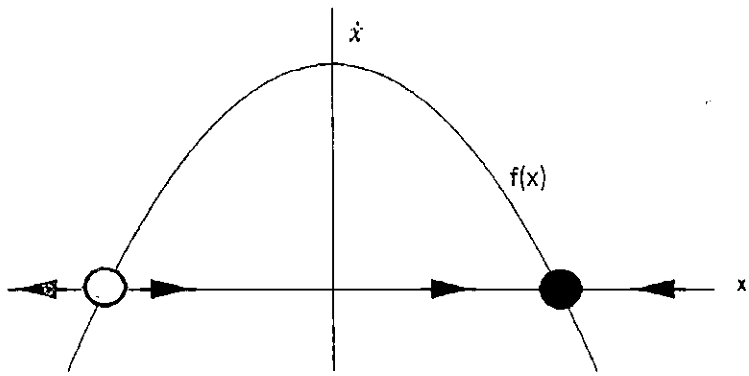

Figure 1.3: Unstable and Stable Fixed Points

To see an example of a *half-stable* fixed point, we look at the following equation: $\dot{x} = -x^2$ and its phase portrait, Figure 1.4. The only fixed point for this equation is when $\mathbf{x}^* = 0$.

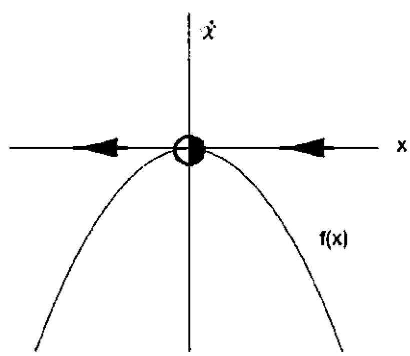

Figure 1.4: Half-Stable Fixed Point

Notice that the flow of f(x) at the origin on either side is going towards the left. This makes the only fixed point at the origin half-stable.

For one-dimensional systems it seems as though a fixed point can be determined to be either stable, unstable, or half-stable. However, there are other types of classifications of fixed points for higher-order dimensions. In the next section. I will go further into this.

1.2 Classification of Fixed Points in Two-Dimensions

For one-dimensional dynamic systems, linear or not, the classification of the fixed point were either unstable, stable or half-stable. What about two-dimensional dynamic systems? Well there is such a classification for them as well.

First, consider a linear system $\dot{\mathbf{x}} = J(\mathbf{x}(t))$, where J is a 2×2 matrix. Suppose J has eigenvalues λ_1, λ_2 with associated eigenvectors $\mathbf{v}_1$, $\mathbf{v}_2$, and that $\mathbf{v}_1$, $\mathbf{v}_2$ is linearly independent. The general solution is $\mathbf{x}(t) = C_1 e^{\lambda_1 t}\mathbf{v}_1 + C_2 e^{\lambda_2 t}\mathbf{v}_2$. (There is a similar formulation in the degenerate case when there is a simple eigenvalue with only a one-dimensional eigenspace, but we will not describe that here). From linear algebra, if $\tau =$ trace(J) = tr(J) and $\Delta =$ determinant(J) = det(J), then the characteristic equation is $\lambda^2 - \tau\lambda + \Delta = 0$, so that its solutions are $\lambda_{1,2} = \dfrac{\tau \pm \sqrt{\tau^2 - 4\Delta}}{2}$.

Now, the rules are as follows. $\tau = \mathrm{tr(J)} = \lambda_1 + \lambda_2$ and $\Delta = \mathrm{det(J)} = \lambda_1\lambda_2$, where λ_1 and λ_2 are the eigenvalues of the matrix J. First, using the determinant gives:

1. If $\Delta < 0$, the eigenvalues are real and have opposite signs making the fixed point a saddle point [Str94].

2. If $\Delta > 0$, the eigenvalues are either real with the same sign, or complex conjugate [Str94].

3. If $\Delta = 0$, at least one of the eigenvalues is zero. Thus, the origin is not an isolated fixed point. There is either a whole line of fixed points or a plane of fixed points if $J = 0$ [Str94].

Second, using the trace can help determine the stability of the fixed point. Assume $\Delta > 0$:

4. If $\tau < 0$ both eigenvalues have negative real parts, so if it is a fixed point, it is stable [Str94].

5. If $\tau > 0$ the eigenvalues are both positive. so if it is a fixed point, it is unstable [Str94].

6. If $\tau = 0$ the fixed point is a neutrally stable center where the eigenvalues are purely imaginary [Str94].

Finally, the discriminant can help determine the classification of the fixed point (again, $\Delta > 0$):

7. If $\tau^2 - 4\Delta > 0$ then it is a node [Str94].

8. If $\tau^2 - 4\Delta < 0$ then it is a spiral [Str94].

9. If $\tau^2 - 4\Delta = 0$ then it is on the borderline. So the fixed point could either be a node, spiral, star node, or degenerate node [Str94].

The following is a helpful diagram that expresses the rules up above:

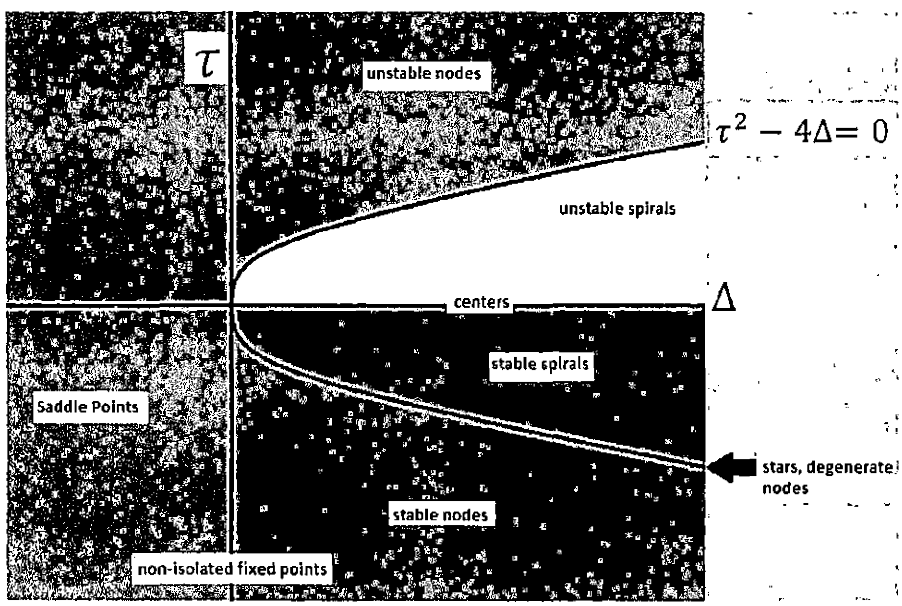

Figure 1.5: Classifications of Fixed Points

The following is a picture showing examples of phase portraits near the different kinds of classifications. Reversing the direction of the arrows in any portrait reverses the stability of the equilibrium point.

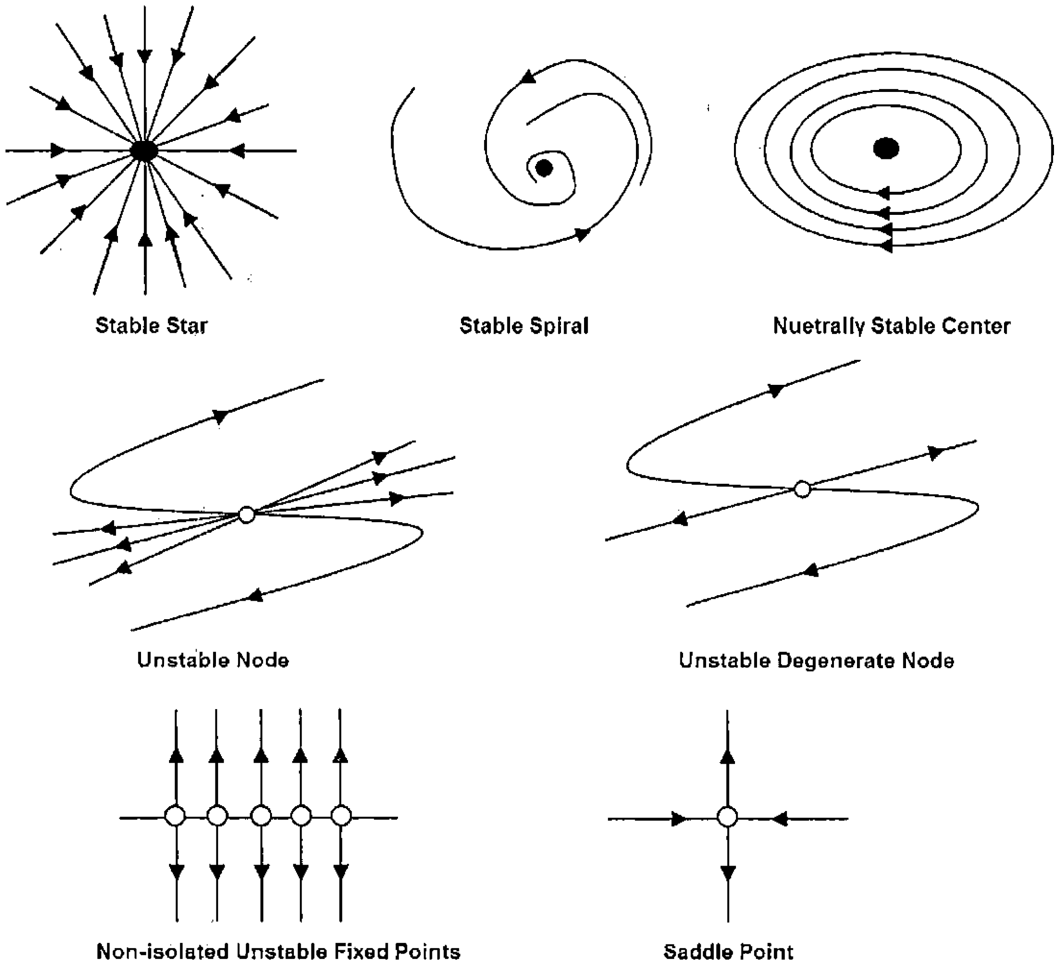

Figure 1.6: Types of Fixed Points for Two-Dimensional Systems

The general solution for a two-dimensional system is given by $\mathbf{x}(t) = C_1 e^{\lambda_1 t}\mathbf{v}_1 + C_2 e^{\lambda_2 t}\mathbf{v}_2$. If λ_1 and λ_2 are complex then so are C_1, C_2, $\mathbf{v}_1$ and $\mathbf{v}_2$, meaning that they each also have complex entries. The complex λ's appear as complex conjugates $\lambda_{\pm} = \alpha \pm i\omega$. Thus, assuming $\omega \neq 0$,

- If $\alpha = \mathrm{Re}(\lambda) < 0$ then the solution is exponentially decaying, so the fixed points are the limit points of stable spirals [Str94].

- If $\alpha = \mathrm{Re}(\lambda) > 0$ then the solution is exponentially growing, so the fixed points are the limit points of unstable spirals [Str94].

- If $\alpha = 0$ then all the solutions are periodic [Str94].

Now, let's recall Figure 1.3 and Figure 1.4. If we looked closely at both of them, we can see their phase portraits were created almost by the same equation. Figure 1.3 had the equation $\dot{x} = 1 - x^2$ while Figure 1.4 had the equation $\dot{x} = -x^2$. Both these equations have $-x^2$ but only differ in their parameter, one being '0' and the other '1'. Well, this is not a mere coincidence. I actually chose these equations on purpose for a specific reason. Although it cannot be seen clearly at the moment, I will begin by saying this: Fixed points can be either created, destroyed, or can change their nature, as some parameters on the dynamics are changed. This kind of qualitative changes in the dynamics are called bifurcations, in which I will go into further detail on the next chapter.

What about non-linear systems? Fixed points can still be found as before, but now we need to classify them by means of linearization. The *linearization* of the system $\dot{\mathbf{x}}(t) = \mathbf{f}(\mathbf{x}(t))$ at the fixed point found by taking its Jacobian

$$J = \begin{pmatrix} \frac{\partial f_1}{x_1} & \frac{\partial f_1}{x_2} & \cdots & \frac{\partial f_1}{x_n} \\ \frac{\partial f_2}{x_1} & \frac{\partial f_2}{x_2} & \cdots & \frac{\partial f_2}{x_n} \\ \vdots & \vdots & \ddots & \vdots \\ \frac{\partial f_m}{x_1} & \frac{\partial f_m}{x_2} & \cdots & \frac{\partial f_m}{x_n} \end{pmatrix}, \qquad \mathbf{f} = \begin{pmatrix} f_1 \\ f_2 \\ \vdots \\ f_n \end{pmatrix}.$$

If J is the Jacobian of the vector function at a fixed point $\mathbf{x}^*$, the linearization of $\dot{\mathbf{x}}(t) = \mathbf{f}(\mathbf{x}(t))$ at $\mathbf{x}^*$ is $\frac{d}{dt}(\dot{\mathbf{x}}(t) - \mathbf{x}^*) = J(\mathbf{x}(t) - \mathbf{x}^*)$.

We classify a non-linear fixed point by looking at the linearization and using the rules mentioned above. Then the fixed point generally has the <u>*same*</u> classification even in the non-lienar system. However, we have to be careful with the border-line cases (e.g. stars or centers): they may become one of the neighboring behaviors in the non-linear system.

To better understand these rules, I will show an example. Lets find the fixed points and classify them of the following nonlinear dynamic system:

$$\begin{aligned} \dot{x} &= 1 + y - e^{-x} \\ \dot{y} &= x^3 - y. \end{aligned}$$

Setting $\dot{x} = 0$ and $\dot{y} = 0$ we get only one fixed point, $(x^*, y^*) = (0, 0)$. Finding its Jacobian:

$$\begin{pmatrix} e^{-x} & 1 \\ 3x^2 & -1 \end{pmatrix}_{(x^*,y^*)}.$$

Then, the Jacobian at the fixed point $(x^*, y^*) = (0, 0)$ is:

$$\begin{pmatrix} e^{-x} & 1 \\ 3x^2 & -1 \end{pmatrix}_{(0,0)} = \begin{pmatrix} 1 & 1 \\ 0 & -1 \end{pmatrix}.$$

The eigenvalues are $\lambda_1 = 1$ and $\lambda_2 = -1$. Thus,

$$\begin{aligned} \tau &= 1 + (-1) &= 0 \\ \Delta &= (1)(-1) &< 0 \\ \tau^2 - 4\Delta &= 0 - 4(-1) &> 0. \end{aligned}$$

Hence, the fixed point $(0, 0)$ is a saddle point. Its phase portrait is the following:

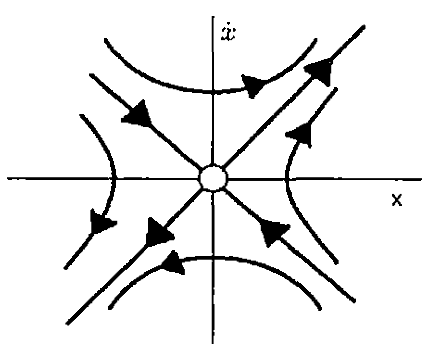

Figure 1.7: Saddle Point Phase Portrait

Chapter 2

Bifurcations

2.1 Introduction

A *Bifurcation* is defined to occur when, upon changing some parameter of the system, a fixed point is created, destroyed, or can change its nature. Bifurcations provide models of transitions and instabilities as some parameter of the system is varied.

One way to think about this is as follows: Suppose I am standing on top of a flexible vertical styrofoam that does not compress and it can support my weight, so it is stable. Now, lets say I somehow gain weight that then the flexible vertical styrofoam becomes unstable and can no longer support my weight. Thus it might bend to the left or to the right in order to compensate for my additional weight.

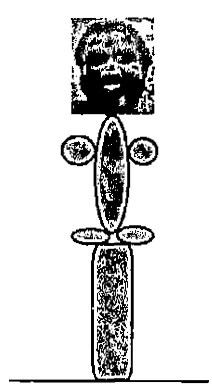

Figure 2.1: My Weight Being Supported

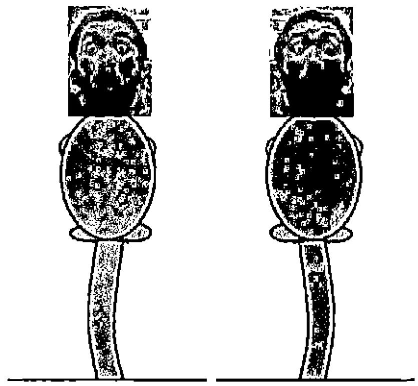

Figure 2.2: My Increased Weight No Longer Being Supported

For one-dimensional dynamical systems there exist saddle-node, transcritical, and pitchfork bifurcations. For phase portraits of two-or-more-dimensional dynamical systems we have new types, such as the Hopf Bifurcation.

2.2 Saddle-Node Bifurcation

A *saddle-Node Bifurcation* occurs when fixed points are either created or destroyed. A general representation of a saddle-node bifurcation is of the form $\dot{x} = r + x^2$ or $\dot{x} = r - x^2$. To see this lets us look at $\dot{x} = x^2 + r$. Looking at Figure 2.3 we can see what happens as the parameter r varies.

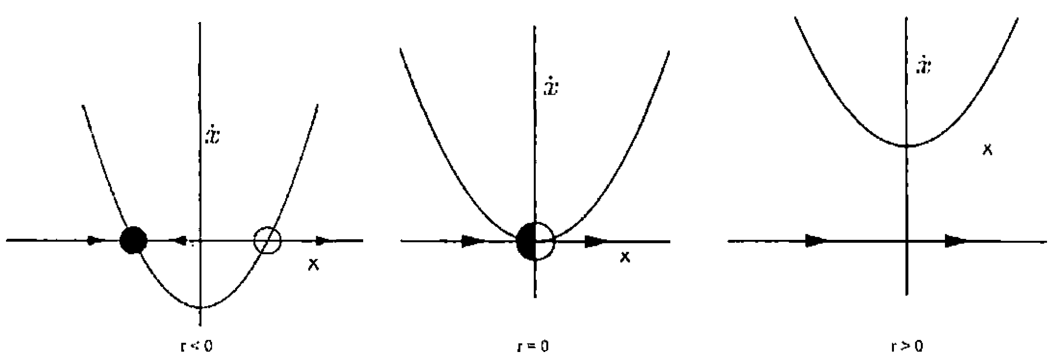

Figure 2.3: Saddle-Node Bifurcation

When $r < 0$, their exist two fixed points, one stable and the other unstable. A saddle-node bifurcation occurs when $r = 0$ and the two fixed points come towards one another and coalesce, giving a half-stable fixed point. Finally, when $r > 0$, the fixed point is destroyed.

A *bifurcation diagram* is the graph of the fixed points x^* vs. r. It shows for what values of r fixed points occur and indicates their stability. The saddle-node bifurcation is pictured in Figure 2.4, the dotted lines show where it is unstable and the solid line shows where it is stable.

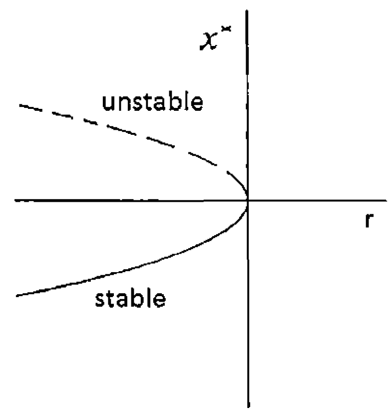

Figure 2.4: Saddle-Node Bifurcation Diagram

Now, recall the previous equations I introduced in Chapter 2, $\dot{x} = -x^2$ and $\dot{x} = 1 - x^2$. It actually turns out that this equation follows the general representation of the saddle-node bifurcation $\dot{x} = r - x^2$. So there was a reason to why I chose these equations. For the equations that I chose, the parameter r varies from 0 to 1, creating two fixed points. Hence, we have a saddle-node bifurcation as in Figure 2.5.

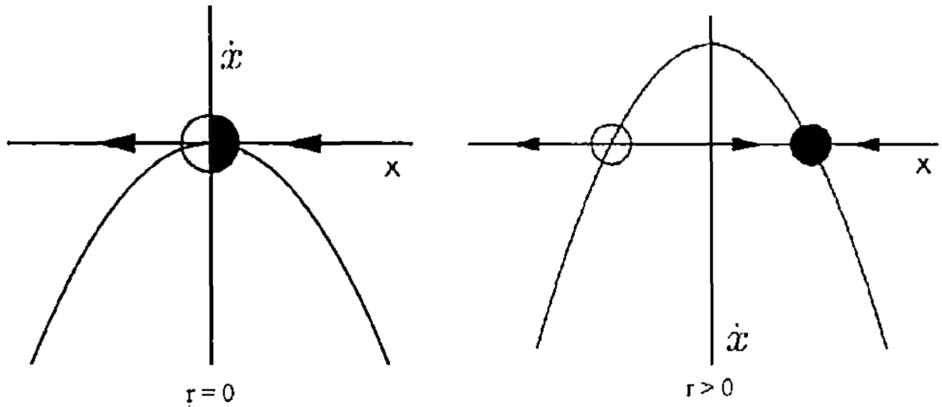

Figure 2.5: Saddle-Node Bifurcation of Example

2.3 Transcritical Bifurcation

A *Transcritical Bifurcation* is when there exists a fixed point that cannot be destroyed; however, it can change its nature of stability. The normal form of it is $\dot{x} = rx - x^2$ or $\dot{x} = rx + x^2$ [Str94]. To better understand this, lets look at $\dot{x} = rx - x^2$.

For $\dot{x} = rx - x^2$, when $r < 0$ their exist two fixed points, one unstable and the other stable. The stable fixed point is actually at the origin. Lets keep this in mind. As the parameter r varies we will see what happens. When $r = 0$, the unstable fixed point of the left-hand side of the origin comes towards the stable fixed point at the origin to create a half-stable fixed point at the origin now. So far, the fixed point at the origin has not been destroyed. Finally, as $r > 0$ another fixed point is created on the right-hand side of the origin, this time being stable while the origin changes its nature of stability to unstable [Str94].

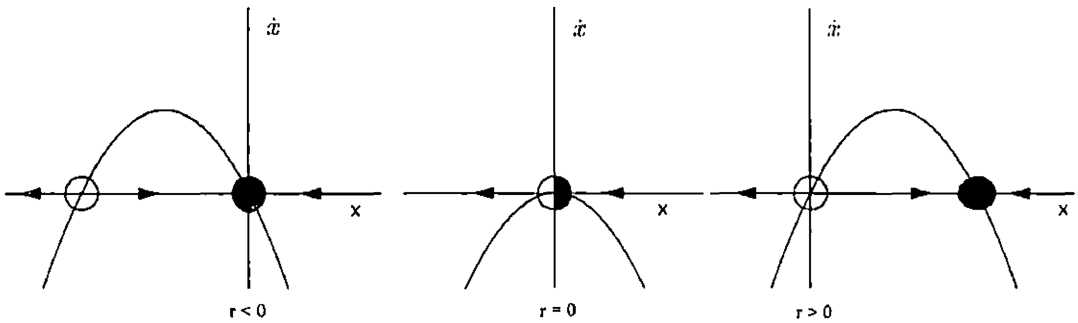

Figure 2.6: Transcritical Bifurcation

Thus, Figure 2.6 shows that the fixed point at the origin cannot be destroyed as the parameter r varies. However, its change of nature can be clearly seen as it becomes stable to half-stable to unstable as r varies. Figure 2.7 shows its bifurcation diagram.

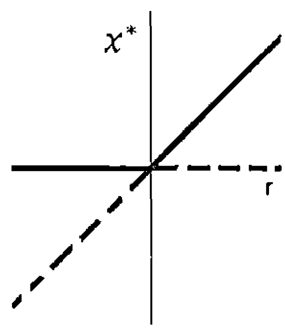

Figure 2.7: Transcritical Bifurcation Diagram

2.4 Pitchfork Bifurcation

Recall how I gained weight and the styrofoam became unstable and it bent either direction to compensate for my extra weight creating symmetric bends. Well, what occured was pitchfork bifurcation. A *pitchfork bifurcation* occurs when a parameter is varied when a single fixed point turns into symmetrically, located on the x-axis, fixed points, (recall what happened when I gained weight and the styrofoam bent on either of two sides). There are two types of pitchfork bifurcations: *supercritical* and *subcritical*.

First, the supercritical pitchfork bifurcation has the normal form $\dot{x} = rx - x^3$.

If $r < 0$ then their exist a stable fixed point. When $r = 0$ the fixed point is still stable, but not as strong as when $r < 0$. However, when $r > 0$, the fixed points splits into three fixed points, a pair of symmetric stable fixed points and one unstable fixed point [Str94], Figure 2.8.

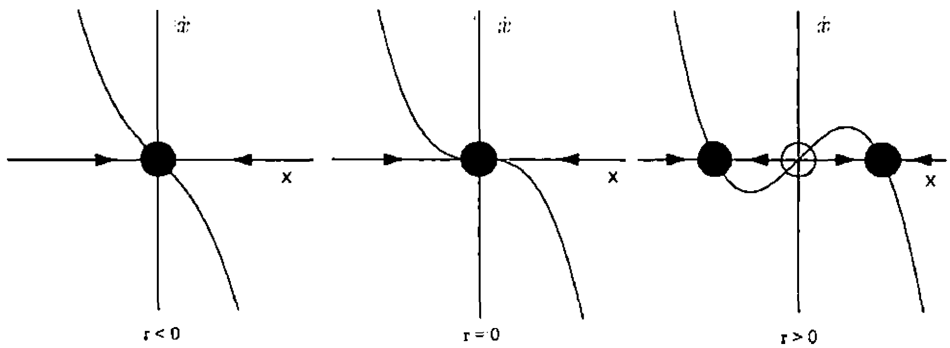

Figure 2.8: Supercritical Pitchfork Bifurcation

The normal form of the subcritical pitchfork bifurcation is $\dot{x} = rx + x^3$ [Str94]. Its behavior as r varies is very similar to that of the supercritical pitchfork bifurcation. One difference is that the stabiltiy of the fixed points are opposite. Its phase potraits are shown in Figure 2.9.

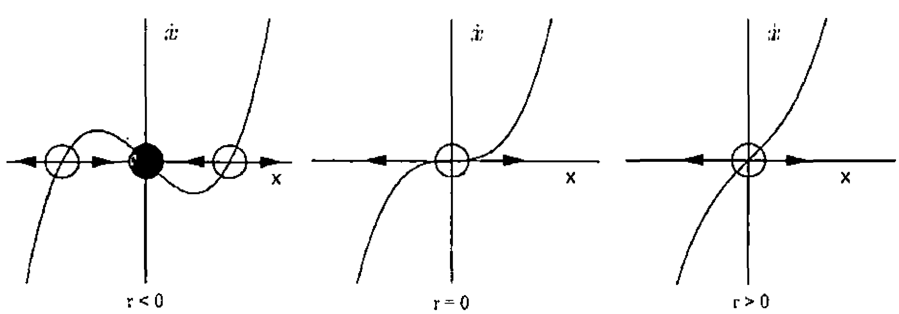

Figure 2.9: Subcritical Pitchfork Bifurcation

The bifurcation diagram of the supercritical and subcritical pitchfork bifurcations are as follows

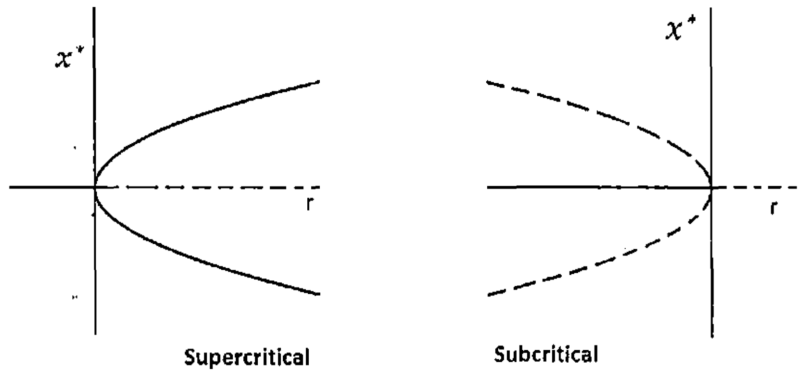

Figure 2.10: Supercritical and Subcritical Pitchfork Bifurcation Diagrams

Figure 2.10 shows that their bifurcation diagrams are mirror opposites of one another, except that where the supercritical is stable, the subcritical is unstable and vice versa.

Before I can continue to Hopf Bifurcations, I need first to mention Limit Cycles. *Limit Cycles* are isolated closed trajecories. Neighboring trajectories are not closed and they spiral either toward or away from the limit cycle [Str94].

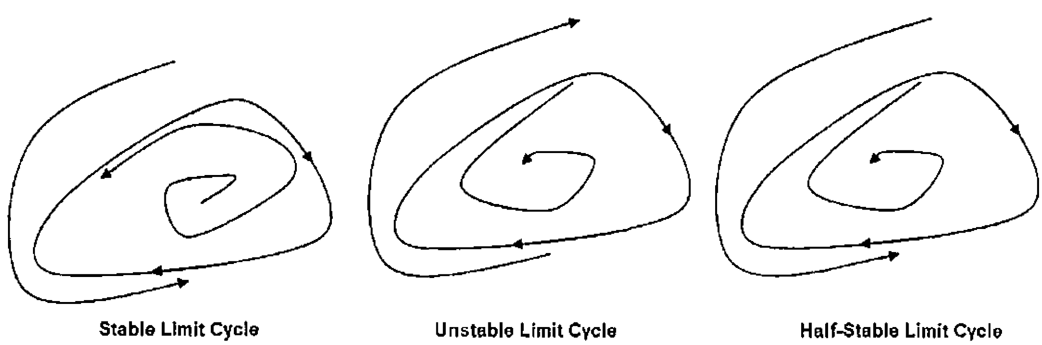

Figure 2.11: Limit Cycles

2.5 Hopf Bifurcation

As stated before, *Hopf Bifurcations* occur in the phase portraits of two-or-more dimensional non-linear systems. They occur when the eigenvalues are of the form $\lambda_1 = \mu + i\omega$ and $\lambda_2 = \mu - i\omega$, with $\omega \neq 0$, and μ changes sign as a parameter is varied (i.e., that the real part of the eigenvalue can change while the imaginary part has to be nonzero). At the critical value of that parameter, $\mu = 0$. If μ is negative then the eigenvalues will be located on the left-hand side of the imaginary axis (see Figure 2.12(a)) and the corresponding solutions will decay exponentially. When μ becomes positive, bothe eigenvalues will cross the imaginary axis to the right-hand side, see figure 2.12(b), and the correspoding solutions will grow exponentially. When μ is equal to zero, there will be a limit cycle. This behavior of crossing the imaginary axis is what causes the limit cycle to either appear or dissapear, depending on the equations. Also, this is what causes the change of stability of the fixed point.

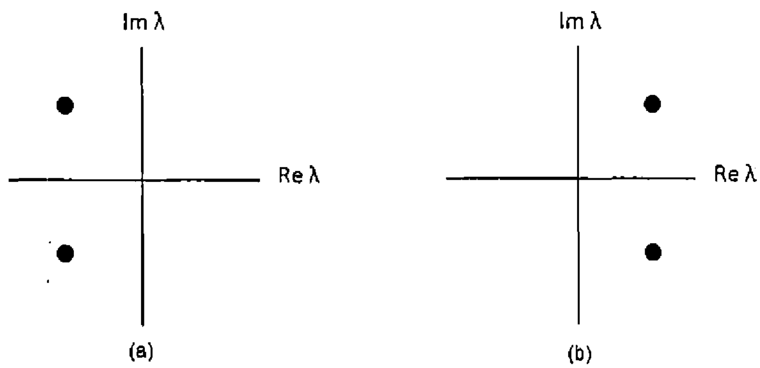

Figure 2.12: Crossing the Imaginary Axis

As with pitchfork bifurcations, Hopf Bifurcations also have a supercritical and subcritical versions.

The *supercritical Hopf Bifurcation* occurs when a stable spiral becomes an unstable spiral with a limit cycle at a critical value. Now suppose the eigenvalues are $\lambda = \mu \pm i\omega$, then the rules of thumb [Str94] for supercrtical Hopf Bifurcations are

- The size of the limit cycle grows continuously from zero, and increases proportional to $\sqrt{\mu - \mu_c}$, for μ close to μ_c .
- The frequency of the limit cyle is given approximately by ω.

The following is an example of a supercritical Hopf Bifurcation. We will look at the following equations and show that when $\mu = 0$, the stable spiral will become and unstable spiral. Consider the following example from Castello [Cas05],

$$\begin{aligned}\dot{x} &= y + \mu x - xy^2 \\ \dot{y} &= \mu y - x + y^3.\end{aligned}$$

Taking its Jacobian,

$$J = \begin{pmatrix} \mu + y^2 & 1 - 2xy \\ -1 & \mu - 3y^2 \end{pmatrix}_{(x^*, y^*)}.$$

The Hopf Bifurcation occurs at the origin, so we will let $(x^*, y^*) = (0, 0)$. Thus,

$$J = \begin{pmatrix} \mu & 1 \\ -1 & \mu \end{pmatrix}_{(0,0)}.$$

Hence, we have $\tau = 2\mu$, $\Delta = \mu^2 + 1$, and $\lambda_{1,2} = \mu \pm i$. So when $\mu < 0$ then, we have that $\tau < 0$, $\Delta > 0$, and $\tau^2 - 4\Delta < 0$. Hence (recall Figure 1.5) the origin, (0,0), is a stable spiral.

When $\mu = 0$, we have $\tau = 0$, $\Delta > 0$, and $\tau^2 - 4\Delta < 0$. The stable spiral starts becoming an unstable spiral, as predicted, with a limit cycle sorrounding it at the critical value. Finally, when $\mu > 0$ we start to see the unstable spiral at the origin. The following illustrations show phase portraits when $\mu = -2$, $\mu = 0$, and $\mu = 2$.

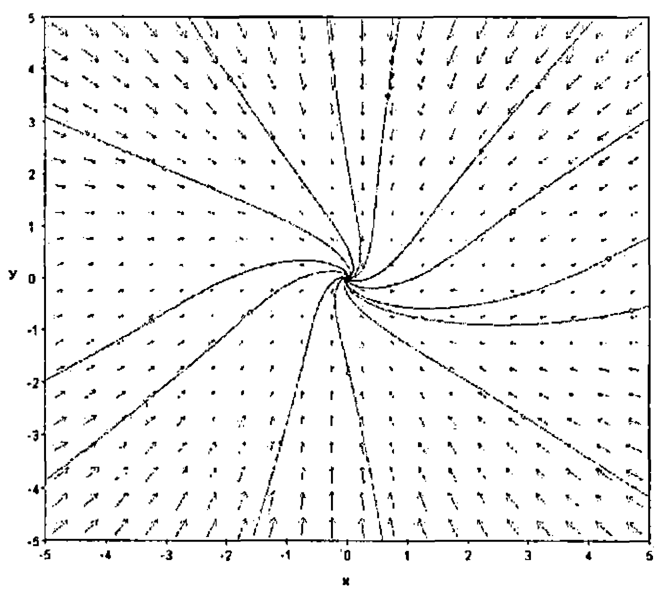

Figure 2.13: Supercritical Hopf Bifurcation at $\mu = -2$

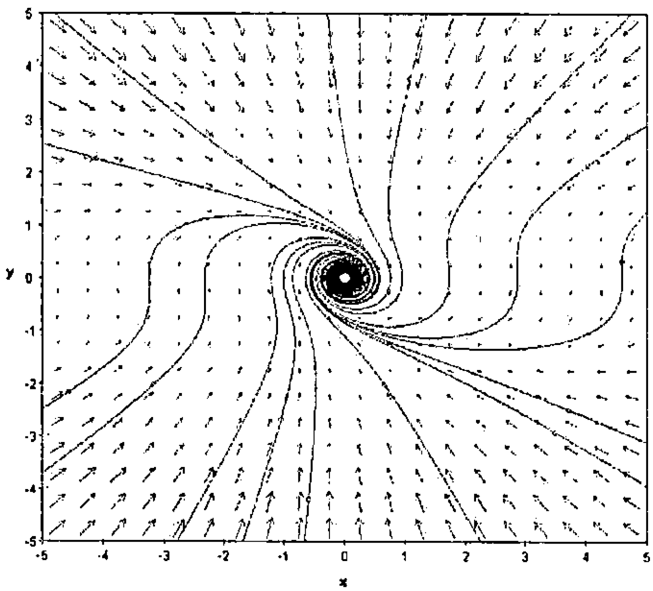

Figure 2.14: Supercritical Hopf Bifurcation at $\mu = 0$

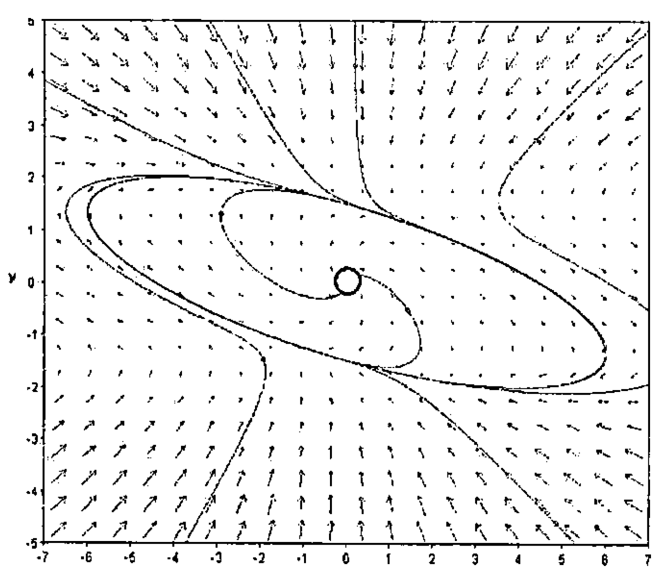

Figure 2.15: Supercritical Hopf Bifurcation at $\mu = 2$

A *subcritical Hopf Bifurcation* occurs when we have an unstable cycle inside a stable limit cycle that then shrinks and engulfs a stable fixed point changing it to an unstable fixed point. This is illustrated in Figure 2.12.

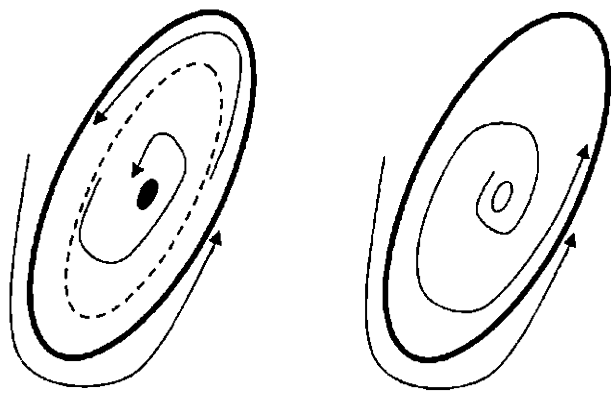

Figure 2.16: Subcritical Hopf Bifurcation

The following is an example, from Clark [CJ09], of a subcrtical Hopf Bifurcation

$$\dot{x} = -y + x^3 - x^5 - 2x^3y^2 + y^2x - y^4x + \mu(x - x^3 - y^2x)$$
$$\dot{y} = x + yx^2 - yx^4 - 2x^2y^3 + y^3 - y^5 + \mu(y - x^2y - y^3).$$

Taking its Jacobian at its critical value (0.0). the origin, we get

$$\begin{pmatrix} \mu & -1 \\ 1 & \mu \end{pmatrix}_{(0,0)}.$$

So $\tau = 2\mu$ and $\Delta = \mu^2 + 1$. As $\mu < 0$, then $\tau < 0$, $\tau^2 - 4\Delta < 0$, and $\Delta > 0$. Thus we have a stable spiral at the critical value. However there exists an unstable limit cycle around the critical value (see Figure 2.17).

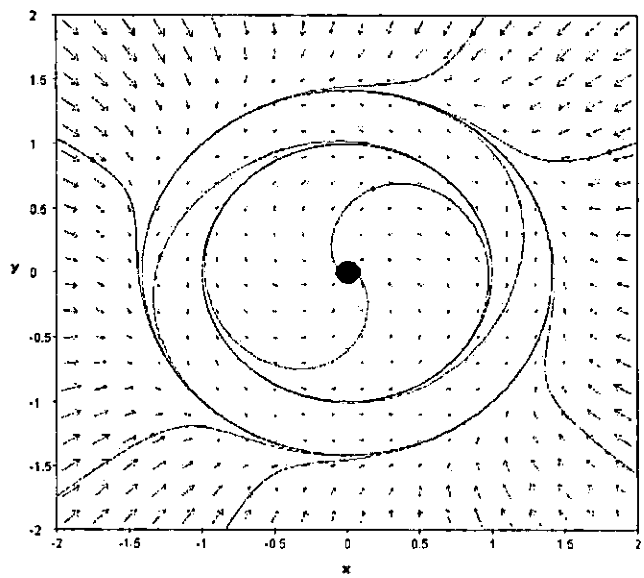

Figure 2.17: Subcritical Hopf Bifurcation at $\mu < 0$

When $\mu = 0$, then $\tau = 0$ and $\Delta > 0$. Thus, we start to see that the unstable limit cycle engulfing the stable point and changing it to an unstable fixed point (see Figure 2.18) as predicted.

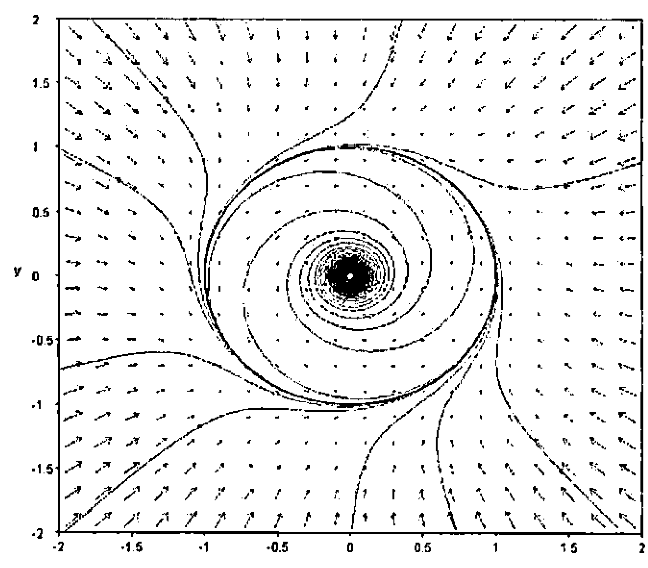

Figure 2.18: Subcritical Hopf Bifurcation at $\mu = 0$

Finaly when $\mu > 0$, then $\tau > 0$ and $\Delta > 0$. Thus, the fixed point has become an unstable spiral.

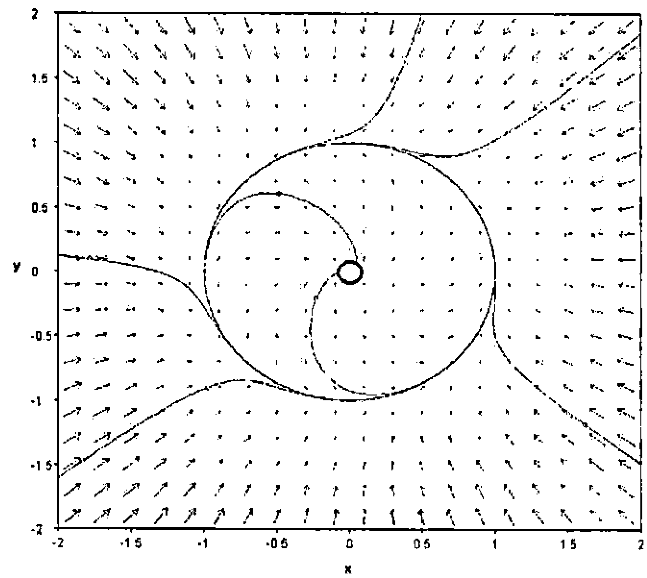

Figure 2.19: Subcritical Hopf Bifurcation at $\mu > 0$

Chapter 3

The Waterwheel Equations

3.1 The Waterwheel

We now have the background knowledge necessary in order to understand The Waterwheel Equations. The following picture of the Waterwheel was created by Willem Malkus and Lou Howard at MIT in the 1970's [Str94].

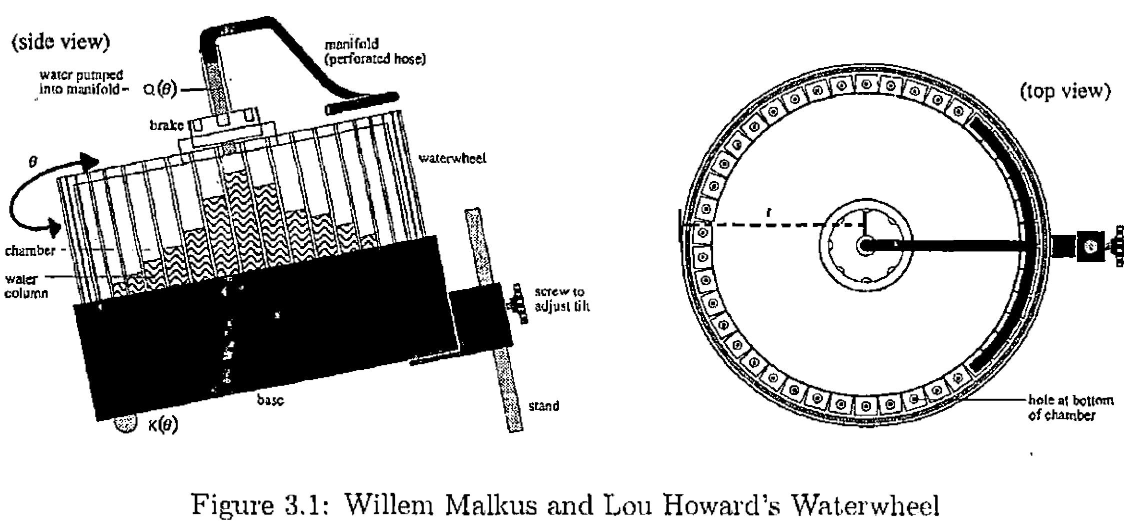

Figure 3.1: Willem Malkus and Lou Howard's Waterwheel

Adapted from Chapter 9 of S.H. Strogatz. *Nonlinear Dynamics and Chaos: with applications to Physics, Biology, Chemistry, and Engineering.* Perseus Books Publishing, Cambridge, Maryland, 1994.

A simplified picture of the situation (and in fact the version of the waterwheel constructed) is in Figure 3.2

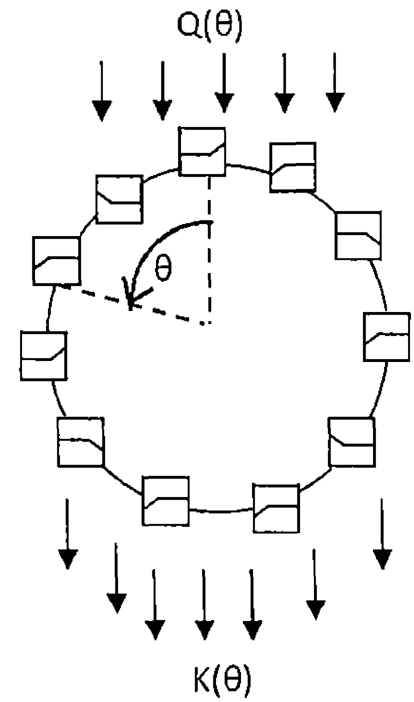

Figure 3.2: Simplified Waterwheel

Let θ be the angular position on the wheel (from 0 to 2π). In Figure 3.2 it can be seen that as the water flows from the top, it slowly leaks out from the bottom of each chamber as the wheel spins either to the left or right. We define Q(θ) to be the flow rate of water into the cups at position θ, and K to be the leakage rate of water out of small holes in each cup. Other parameters of the wheel are r, the radius of the wheel, and v, the rotational damping rate of the wheel, due to friction at the center.

3.2 Parameters and Variables of The Waterwheel

There are three variables that describe the state of the waterwheel: $\omega(t)$ is the angular velocity of the wheel, $m(\theta, t)$ is the mass density of water around the rim of the wheel (the mass between θ_1 and θ_2 is therefore $M(t) = \int_{\theta_1}^{\theta_2} m(\theta, t) d\theta$), and I is the moment of inertia of the wheel [Str94].

Let us look at a small section of the rim of the waterwhel as in Figure 3.3.

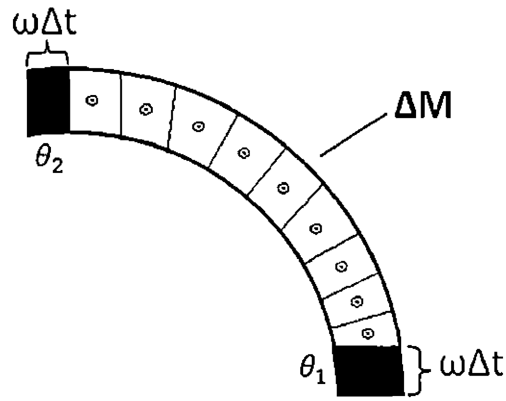

Figure 3.3: Section of the Rim of the Waterwheel

I want to know the change in the mass of water, ΔM, on the interval from θ_1 to θ_2 in a small interval Δt of time. Then the change in mass is

$$\Delta M = \Delta t\Big(\int_{\theta_1}^{\theta_2} Q d\theta - \int_{\theta_1}^{\theta_2} Km d\theta\Big) + m(\theta_1)\omega\Delta t - m(\theta_2)\omega\Delta t. \tag{3.1}$$

The part of the equation that describes the mass of water entering and exiting the segment due to the motion of the wheel is

$$m(\theta_1)\omega\Delta t - m(\theta_2)\omega\Delta t = \omega\Delta t[m(\theta_1) - m(\theta_2)].$$

Note that, $\int_{\theta_1}^{\theta_2} \frac{\partial m}{\partial \theta} d\theta = m(\theta_2) - m(\theta_1)$. So, $m(\theta_1) - m(\theta_2) = -\int_{\theta_1}^{\theta_2} \frac{\partial m}{\partial \theta} d\theta$. Thus substituting it into equation (3.1),

$$\Delta M = \Delta t \int_{\theta_1}^{\theta_2} \Big(Q - Km - \omega\frac{\partial m}{\partial \theta}\Big) d\theta,$$

dividing by Δt to both sides and taking the limit as $t \to 0$,

$$\frac{dM}{dt} = \lim_{t \to 0} \frac{\Delta M}{\Delta t} = \int_{\theta_1}^{\theta_2} \Big(Q - Km - \omega\frac{\partial m}{\partial \theta}\Big) d\theta.$$

However, $\frac{dM}{dt} = \frac{d}{dt}\int_{\theta_1}^{\theta_2} m d\theta = \int_{\theta_1}^{\theta_2} \frac{\partial m}{\partial t} d\theta$. Thus,

$$\int_{\theta_1}^{\theta_2} \frac{\partial m}{\partial t} d\theta = \int_{\theta_1}^{\theta_2} \Big(Q - Km - \omega\frac{\partial m}{\partial \theta}\Big) d\theta.$$

This is true for all θ_1 and θ_2. Thus,

$$\frac{\partial m}{\partial t} = Q - Km - \omega\frac{\partial m}{\partial \theta}. \tag{3.2}$$

Equation (3.2) is known as *continuity equation.*

Now, we need to describe $\omega(t)$ as it changes with time. The total torque is expressed by

$$I\dot{\omega} = -v\omega + gr\int_0^{2\pi} m(\theta, t)\sin\theta d\theta, \tag{3.3}$$

$-v\omega$ is the damping torque, where $v > 0$ (the negative sign indicates that the damping opposes the motion); and $gr\int_0^{2\pi} m(\theta, t)\sin\theta d\theta$ is the gravitational torque due to the mass of water in the wheel, where g is related to the gravitational constant. Equation (3.3) is refered to as the *Integro-differential equation.*

But what of out third variable, I, the moment of inertia? Well, we can ignore it over time, because of the following:

Theorem 3.1. *$I(t)$ becomes constant as $t \to \infty$.*

Proof. The total moment of inertia is a sum $I = I_{wheel} + I_{water}$, where I_{wheel} depends only on the apparatus, and not on the distribution of water around the rim.

- First, we need to express I_{water} in term of $M = \int_0^{2\pi} m(\theta, t)d\theta$. The moment of inertia of a continuous circular solid of negligible thickness rotating about a known axis is given by

$$I = \int_0^{2\pi} \rho(\theta)r^2 d\theta,$$

where, r is the radius vector of a point within the body, $\rho(\theta)$ is the mass density at point θ, and r is the distance from the axis of rotation. So, it follows that

$$I_{water} = \int_0^{2\pi} m(\theta, t)r^2 d\theta = r^2\int_0^{2\pi} m(\theta, t)d\theta = r^2 M.$$

- Second, we must show that M satisfies $\dot{M} = Q_{total} - KM$, where $Q_{total} = \int_0^{2\pi} Q(\theta)d\theta$.

Recall $M = \int_0^{2\pi} m(\theta,t)d\theta$ and Equation (4.2) $\frac{\partial m}{\partial t} = Q - Km - \omega\frac{\partial m}{\partial \theta}$.

$$\begin{aligned} So,\ \dot{M} &= \int_0^{2\pi} \frac{\partial m}{\partial t} d\theta \\ &= \int_{\theta_1}^{\theta_2} \left(Q - Km - \omega\frac{\partial m}{\partial \theta}\right) d\theta \\ &= \int_0^{2\pi} Q d\theta - K\int_0^{2\pi} m d\theta - \omega\int_0^{2\pi} \frac{\partial m(\theta,t)}{\partial \theta} d\theta \\ &= Q_{total} - KM - \omega[m(2\pi,t) - m(0,t)] \\ &= Q_{total} - KM - 0. \end{aligned}$$

Thus, $\dot{M} = Q_{total} - KM$.

By separation of variables, it is easily seen that the solution to this equation is

$$\mathrm{M} = \frac{Q_{total} + Ce^{-t}}{K}. \tag{3.4}$$

Note, that $e^{-t} \to 0$ as $t \to \infty$. Hence, $M \to \frac{Q_{total}}{K}$ as $t \to \infty$.
Using (3.4), we see that

$$\begin{aligned} \lim_{t\to\infty} I(t) &= \lim_{t\to\infty} \left[I_{wheel} + r^2 M\right] \\ &= \lim_{t\to\infty} I_{wheel} + r^2\frac{Q_{total}}{K}. \end{aligned}$$

Since, I_{wheel} depends only on the apparatus itself: I_{wheel} is constant! Hence,

$$\lim_{t\to\infty} I(t) = I_{wheel} + r^2\frac{Q_{total}}{K}.$$

$\square$

Thus, it has been shown that $I(t)$ approaches a constant as $t \to \infty$.

The next section will use the continuity equation (3.2) and the Integro-differential equation (3.3) to obtain *The Waterwheel Equations.*

3.3 The Waterwheel Equations

We may reasonably assume that m and Q are smooth so they have Fourier expansions:

$$m(\theta,t)=\sum_{n=0}^{\infty}[a_n(t)\sin n\theta+b_n(t)\cos n\theta]$$
$$Q(\theta)=\sum_{n=0}^{\infty}q_n\cos n\theta.$$

Here Q is assume to be a even function, hence it only has a cosine series. Now,
$\frac{\partial m}{\partial t}=\frac{\partial}{\partial t}\Big(\sum_{n=0}^{\infty}[a_n(t)\sin n\theta+b_n(t)\cos n\theta]\Big)=\sum_{n=0}^{\infty}[\dot{a}_n(t)\sin n\theta+\dot{b}_n(t)\cos n\theta]$, and
$\frac{\partial m}{\partial \theta}=\frac{\partial}{\partial \theta}\Big(\sum_{n=0}^{\infty}[a_n(t)\sin n\theta+b_n(t)\cos n\theta]\Big)=\sum_{n=0}^{\infty}n[a_n(t)\cos n\theta-b_n(t)\sin n\theta]$.

It then follows from the continuity equation 3.2, that

$$\frac{\partial m}{\partial t}=Q-Km-\omega\frac{\partial m}{\partial \theta}$$
$$\sum_{n=0}^{\infty}[\dot{a}_n(t)\sin n\theta+\dot{b}_n(t)\cos n\theta]=\sum_{n=0}^{\infty}q_n\cos n\theta-K\Big(\sum_{n=0}^{\infty}[a_n(t)\sin n\theta+b_n(t)\cos n\theta]\Big)$$
$$-\omega\Big(\sum_{n=0}^{\infty}n[a_n(t)\cos n\theta-b_n(t)\sin n\theta]\Big).$$

Equating coefficients in the orthogonal basis $\{\sin n\theta,\cos n\theta,n=0,1,2,\dots\}$, we have

$$\begin{aligned}\dot{a}_n&=-Ka_n+n\omega b_n\\ \dot{b}_n&=q_n-Kb_n-n\omega a_n.\end{aligned}\tag{3.5}$$

Which are the first two of the three Waterwheel equations. Recall equation (3.3), the *Integro-differential equation*

$$I\dot{\omega}=-v\omega+gr\int_0^{2\pi}m(\theta,t)\sin\theta d\theta.$$

Dividing both sides by I and using the Fourier Expansions for $m(\theta,t)$ we have the following,

$$\dot{\omega} = \frac{-v\omega + gr \displaystyle\int_0^{2\pi} \sum_{n=0}^{\infty} [a_n(t)\sin n\theta + b_n(t)\cos n\theta] \sin\theta d\theta}{I},$$

applying orthogonality again leaves us with,

$$\dot{\omega} = \frac{-v\omega + gr \displaystyle\int_0^{2\pi} a_1 \sin^2\theta d\theta}{I} = \frac{-v\omega + \pi g r a_1}{I}. \tag{3.6}$$

This is the third equation in the system of equations of The Waterwheel. The $n = 1$ mode gives the waterwheel equations. So, why do we ignore higher-order modes and n = 0 mode?

The $n = 0$ mode can be ignored since a_0 can be taken to be 0 as $\sin(n\theta) = 0$ for $n = 0$ and $b_0 = 0$ as there is no constant part of the water content of the wheel.

Now consider $n > 1$ in

$$\begin{aligned} \dot{a}_n &= n\omega b_n - K a_n \\ \dot{b}_n &= -n\omega a_n - K b_n. \end{aligned}$$

Letting,

$$\mathbf{a}_n(t) = \begin{pmatrix} \dot{a}_n \\ \dot{b}_n \end{pmatrix} = \begin{pmatrix} -K & n\omega \\ -n\omega & -K \end{pmatrix} \begin{pmatrix} a_n \\ b_n \end{pmatrix}.$$

and finding their eigenvalues by $det(\mathbf{a}_n - \lambda I) = 0$ we get $\lambda^2 + 2K\lambda + (K^2 + [n\omega]^2) = 0$. Thus, $\lambda_{1,2} = -K \pm in\omega$. The eigenvectors satisfy

$$(\mathbf{a}_n - \lambda_{1,2} I) \begin{pmatrix} a_n \\ b_n \end{pmatrix} = \begin{pmatrix} in\omega & n\omega \\ -n\omega & -in\omega \end{pmatrix} \begin{pmatrix} a_n \\ b_n \end{pmatrix} = 0,$$

which has linearly independent solutions

$$\begin{pmatrix} 1 \\ i \end{pmatrix} \; and \; \begin{pmatrix} 1 \\ -i \end{pmatrix}.$$

Thus,

$$\mathbf{a}_n(t) = C_1 e^{(-K+in\omega)t} \begin{pmatrix} 1 \\ i \end{pmatrix} + C_2 e^{(-K-in\omega)t} \begin{pmatrix} 1 \\ -i \end{pmatrix}.$$

Recall $\alpha = \text{Re}(\lambda_{1,2}) < 0$, so $\mathbf{a}_n$ decays. Hence, $a_n, b_n \to 0$ as $t \to \infty$. This is why we ignore higher-order modes.

Therefore, the only mode we care about is when $n = 1$, giving us the three Waterwheel equations,

$$\begin{aligned} \dot{a}_1 &= \quad \omega b_1 - K a_1 \\ \dot{b}_1 &= -\omega a_1 - K b_1 + q_1 \\ \dot{\omega} &= \frac{-v\omega + \pi g r a_1}{I}. \end{aligned} \tag{3.7}$$

3.4 Fixed Points of The Waterwheel Equations

We are now going to find the fixed points of the equations in (3.7). These are vectors (a_1, b_1, ω) where $\dot{a}_1, \dot{b}_1$, and $\dot{\omega}$ are all zero. So, let $\dot{a}_1 = 0$, $\dot{b}_1 = 0$, and $\dot{\omega} = 0$. This gives

$$\begin{aligned} 0 &= \quad \omega b_1 - K a_1 \\ 0 &= -\omega a_1 - K b_1 + q_1 \\ 0 &= \frac{-v\omega + \pi g r a_1}{I}, \end{aligned}$$

solving for a_1 for each one,

$$a_1 = \frac{\omega b_1}{K} \tag{3.8}$$

$$\omega a_1 = q_1 - K b_1 \tag{3.9}$$

$$a_1 = \frac{v\omega}{\pi g r}. \tag{3.10}$$

If $\omega = 0$ then (3.8) and (3.10) give $a_1 = 0$ and (3.9) gives $b_1 = \dfrac{q_1}{K}$ (assuming $K \neq 0$). So, $(a_1^*, b_1^*, \omega^*) = \left(0, \dfrac{\mathbf{q_1}}{\mathbf{K}}, 0\right)$. This fixed point represents the waterwheel at rest. The inflow rate of the water is balanced by the leakage rate of the water.

If $\omega \neq 0$ and $K \neq 0$, solving for a_1 in equation (3.9) and substituting it into (3.8), we get $\dfrac{\omega^2 b_1}{K} = q_1 - K b_1$. Solving for b_1 results in

$$b_1 = \frac{q_1 K}{\omega^2 + K^2}. \tag{3.11}$$

Doing the same thing with (3.8) and (3.10) results in

$$b_1 = \frac{vK}{\pi g r}. \tag{3.12}$$

Substituting (3.11) into (3.12) and dividing by K we get

$$\omega^* = \pm\sqrt{\frac{q_1 \pi g r}{v} - K^2} = \pm K\sqrt{\frac{q_1 \pi g r}{K^2 v} - 1}$$

which then leads to,

$$a_1^* = \frac{\omega b_1}{K} = \frac{\pm v\sqrt{\frac{\pi g r q_1}{v} - K^2}}{\pi g r}.$$

Thus, this results into two fixed points

$$\left(a_1^*, b_1^*, \omega^*\right) = \left(\frac{\pm v\sqrt{\frac{\pi g r q_1}{v} - K^2}}{\pi g r}, \; \frac{vK}{\pi g r}, \; \pm K\sqrt{\frac{q_1 \pi g r}{K^2 v} - 1}\right).$$

These solutions represent when the waterwheel is moving either to the left or to the right in stable rotation. However, we need $\frac{q_1 \pi g r}{K^2 v} > 1$ in order for this to happen. We will see that, as the *Rayleigh number* $\frac{q_1 \pi g r}{K^2 v}$ increases beyond a certain critical value, the flow becomes chaotic, which is what I am curious about. This will be shown when the Waterwheel Equations are converted into the Lorenz Equations. Note that the Rayleigh number increases with the flow rate q_1. As this increases, we will see bifurcations appear.

Chapter 4

The Lorenz Equations

4.1 Introduction

Let us recall The Lorenz Equations that were mentioned in the beginning

$$
\begin{aligned}
\dot{x} &= \sigma(y - x) \\
\dot{y} &= rz - xz - y \\
\dot{z} &= xy - bz.
\end{aligned}
\tag{4.1}
$$

These equations were first realized by *Edward N. Lorenz* in his paper *Deterministic Nonperiodic Flow*. In this paper he used this finite system of deterministic ordinary nonlinear differential equations to represent forced dissipative hydrodynamic flow. Once we convert the Waterwheel Equations (3.7) into the Lorenz Equations, we will see clearly what can lead us to Chaos.

4.2 The Lorenz Equations

Theorem 4.1. *The Waterwheel Equations are equivalent to the Lorenz Equations.*

Proof. Recall the Waterwheel Equations:

$$
\begin{aligned}
\dot{a}_1 &= \omega b_1 - K a_1 \\
\dot{b}_1 &= -\omega a_1 - K b_1 + q_1 \\
\dot{\omega} &= \frac{-v\omega + \pi g r a_1}{I}.
\end{aligned}
$$

We will be converting all the variables: a, b, ω, and t to dimensionless variables. We let $\omega = Ax + B$, $a_1 = Cy + D, b_1 = Ez + F$ and $\tau = Tt$, where A, B, C, D, E and F are yet to be determined constants; and A, C, E, F, and T cannot be zero. Define $\dot{\mathbf{x}} = \frac{d\mathbf{x}}{d\tau} = \frac{d\mathbf{x}}{dt}\frac{dt}{d\tau} = \frac{d\mathbf{x}}{dt}\frac{1}{T}$, where

$$\dot{\mathbf{x}} = \begin{pmatrix} \dot{x} \\ \dot{y} \\ \dot{z} \end{pmatrix}$$

and $\dot{a}_1 = \frac{da_1}{dt}$, $\dot{b}_1 = \frac{db_1}{dt}$, $\dot{\omega} = \frac{d\omega}{dt}$. Taking the derivative of ω, a_1, and b_1 gives $\dot{\omega} = TA\dot{x}$, $\dot{a}_1 = TC\dot{y}$, and $\dot{b}_1 = TE\dot{z}$

Substituting for the indicated variables in the equation $\dot{a}_1 = \omega b_1 - Ka_1$

$$TC\dot{y} = (Ax + B)(Ez + F) - K(Cy + D).$$

Substituting for $\dot{y} = rz - xz - y$ gives

$$TC(Rx - xz - y) = AFx + AExz - KCy + BEz + BF - KD.$$

Equating like coefficients in both sides leads to $T = K$, $R = \frac{AF}{TC}$, $KC = -AE$, $B = 0$ and $D = 0$. Making the new substitutions into the appropriate variables, we now get $\omega = Ax$, $a_1 = Cy$, $b_1 = Ez + F$, and $Kt = \tau$.

Doing similar steps for the second equation, $\dot{b}_1 = -\omega a_1 + q_1 - Kb_1$, we get

$$KE\dot{z} = - ACxy + q_1 - K(EZ + F)$$
$$KE(xy - bz) = - ACxy - KEz + q_1 - KF.$$

Thus, $b = KE = -AC$ and $F = \frac{q_1}{K}$. Recall that $KC = -AE$. Then this leads us to $A = \pm K$ and $E = \mp C$. Now we have $\omega = \pm K^2$, $a_1 = Cy$, $b_1 = \mp Cz + \frac{q_1}{K}$ and $Kt = \tau$

Finally, the third equation $\dot{\omega} = -\frac{v}{I}\omega + \frac{\pi gr}{I}a_1$ results in

$$K^2\dot{x} = \mp\frac{v}{I}Kx + \frac{\pi gr}{I}Cy$$
$$K^2(\sigma y - \sigma x) = -\frac{v}{I}x + \frac{\pi gr}{I}Cy.$$

This leads to $\sigma = \frac{v}{IK}$ and $C = \frac{vK}{\pi gr}$. Recall $R = \frac{AF}{TC} = \frac{q_1 \pi gr}{K^2 v}$, the Rayleigh number. Therefore, letting the change of variables be

$\omega = Kx$, $a_1 = \dfrac{vK}{\pi g r} y$, $b_1 = \dfrac{vK}{\pi g r} z + \dfrac{q_1}{K}$, $\tau = Kt$, and rewriting R as r and substituting these into $\dot{\omega}$, $\dot{a}_1$ and $\dot{b}_1$ we will give us

$$\begin{aligned}\dot{x} =& \quad \sigma(y - x)\\ \dot{y} =& \quad rx - xz - y\\ \dot{z} =& \quad xy - bz.\end{aligned}$$

□

These are the Lorenz Equations! As we found the fixed points of The Waterwheel Equations, we will also find the fixed points The Lorenz Equations.

4.3 Fixed Points of Lorenz Equations

So we begin by setting $\dot{x} = 0$, $\dot{y} = 0$, and $\dot{z} = 0$.

$$0 = \quad \sigma(y - x) \tag{4.3}$$

$$0 = \quad rx - xz - y \tag{4.4}$$

$$0 = \quad xy - bz. \tag{4.5}$$

From the first equation (4.3) we get $\sigma y = \sigma x$. Since, $\sigma > 0$, $x = y$. So (4.4) we get

$$\begin{aligned}0 =& ry - y - yz\\ 0 =& y(r - 1 - z).\end{aligned}$$

This leads us to two different cases: case 1: $y = 0$ and case 2: $z = r - 1$.

- case 1: When $y = 0$, then $x = 0$. Subtituting this into (4.5) results in $0 = bz$. Recall that $b \neq 0$. Thus, $z = 0$. Hence we have the fixed point $(x^*, y^*, z^*) = (0, 0, 0)$ for all r.

- case 2: When $z = r - 1$ and $x = y$, substituting these into (4.5) gives $0 = y^2 - b(r - 1)$. Solving for y, $y = \pm\sqrt{b(r-1)}$. From (4.3) $x = y$. So $x = \pm\sqrt{b(r-1)}$. Thus, we have two more fixed points

$$(x^*, y^*, z^*) = \Big(\pm \sqrt{b(r-1)}, \pm\sqrt{b(r-1)}, r - 1 \Big) \text{ for } r > 1.$$

Notice that x^* and y^* are a symmetrical pair of fixed points. This will give us a pitchfork bifurcation, I will go into this further in the next section as we find the stability of the three fixed points that we have found.

4.4 Stability and Fixed Points of Lorenz Equations

Lets recall the fixed point of case 1: $(x^*, y^*, z^*) = (0,0,0)$. In order to find its stability, we linearize the Lorenz Equations at the origin. However, in this case we can ignore $\dot{z}$. This is because the third equation becomes $\dot{z} = -bz$. The solution of this equation is $z(t) = Ce^{-bt}$ and so $z(t) \to 0$ as $t \to \infty$. The linearization of the remaining Lorenz Equations at the origin is

$$\begin{pmatrix} -\sigma & \sigma \\ r & -1 \end{pmatrix}.$$

It then follows that the trace τ, and its determinant Δ, are

$$\tau = -\sigma - 1 < 0$$
$$\Delta = \sigma(1 - r).$$

Note that Δ leads us to two different scenarios depending on r.

1. $r > 1 \Rightarrow \Delta < 0$; the eigenvalues are of opposite sign and we have a saddle point at (0,0,0).
2. $r < 1 \Rightarrow \Delta > 0$; and $\tau^2 - 4\Delta = (\sigma + 1)^2 - 4\sigma(1 - r) = (\sigma - 1)^2 + 4 > 0$, thus the fixed point (0,0,0) is stable.

Now, for the part that we are more interested in, linearizing at the fixed point $(x^*, y^*, z^*) = \left(\pm\sqrt{b(r-1)}, \pm\sqrt{b(r-1)}, r-1\right)$ for $r > 1$. Lorenz called these fixed points C^+ and C^- [Str94]. To save time and paper, we will see the linearization of only at the fixed point C^+, since doing it at C^- is similar and will result in the same solutions.

Linearizing at C^+ gives the following matrix

$$\begin{pmatrix} -\sigma - \lambda & \sigma & 0 \\ 1 & -1 - \lambda & -\sqrt{b(r-1)} \\ \sqrt{b(r-1)} & \sqrt{b(r-1)} & -b - \lambda \end{pmatrix},$$

we seek its eigenvalues. The characteristic equation is

$$\lambda^3 + (\sigma + 1 + b)\lambda^2 + (\sigma + r)b\lambda + 2b\sigma(r - 1) = 0.$$

Claim 4.2. *For a critical value $r_c > 1$, a Hopf bifurcation occurs, as long as $\sigma > b + 1$.*

To see this, look for purely imaginary solutions in the characteristic equation. Setting $\lambda = i\omega$ we have

$$\begin{aligned} (i\omega)^3 + (\sigma + 1 + b)(i\omega)^2 + (\sigma + r)b(i\omega) + 2b\sigma(r - 1) &= 0 \\ -i\omega^3 - (\sigma + 1 + b)\omega^2 + (\sigma + r)b(i\omega) + 2b\sigma(r - 1) &= 0. \end{aligned}$$

Organizing real and imaginary parts we get

$$-\omega^3 + (rb + b\sigma)\omega = 0 \tag{4.6}$$

$$(\sigma + b + 1)\omega^2 - 2b\sigma(r - 1) = 0. \tag{4.7}$$

Since $\omega \neq 0$, (4.6) is just ω^2 we have $\omega^2 = rb + b\sigma$. Substituting ω^2 into (4.7) gives

$$rb + b\sigma = \frac{2b\sigma(r - 1)}{\sigma + b + 1}.$$

Finally, solving for r, we get the critical value

$$r_c = \frac{\sigma(\sigma + b + 3)}{\sigma - b - 1} \text{ where, } \sigma - b - 1 > 0.$$

In other words, the real parts of the eigenvalues become zero as $r = r_c$. One thing that this thing shows is that the fixed points C^+ and C^- are stables nodes for $1 < r < r_c = \dfrac{\sigma(\sigma + b + 3)}{\sigma - b - 1}$. So while $\sigma < b + 1$ then C^- and C^+ will be stable for all $r_c > r > 0$. Thus, the pair of symmetric fixed points give a supercritical pitchfork bifurcation. Their stability is lost at r_c. Hence, a Hopf Bifurcation has occured, a subcritical Hopf bifurcation at that. A demonstration of this fact is provided in Drazin's book, [Dra92].

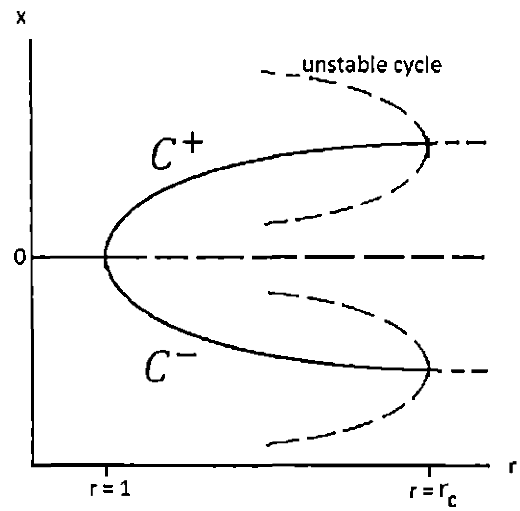

Figure 4.1: Bifurcation Diagram of C^+ and C^-

We will see in the next chapter that if we go beyond the critical value, r_c, then Chaos occurs.

Chapter 5

Chaos

5.1 Choatic Behavior of The Waterwheel Equations

Chaos is defined as a aperiodic long term behavior in a deterministic system that exhibits sensitive dependence on initial conditions [Str94]. To better understand this, I will begin with the critical value of the Lorenz equation

$$r_c = \frac{\sigma(\sigma + b + 3)}{\sigma - b - 1} \ .$$

For example $r_c = \frac{470}{19} \approx 24.74$ when $\sigma = 10$ and $b = \frac{8}{3}$ [Lor63]. Hence, anything above r_c will have a chaotic behavior. This can be seen when plotting the solutions to the initial condition $(0, 1, 0)$ on a y vs. t plane. This can be seen in Figure 5.1.

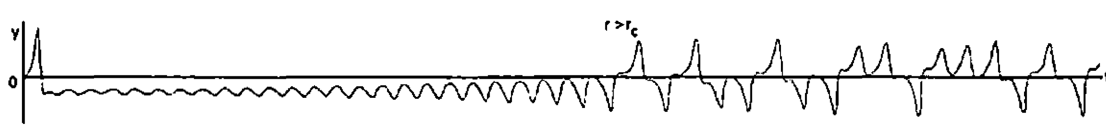

Figure 5.1: Aperiodic Behavior
Adapted from page 137, volume 20, of Deterministic nonperiodic flow. *Journal of the Atmospheric Science: Deterministic Nonperiodic Flow*. 1963.

From the graph above we can see that the system at $r > r_c$ begins with a seemingly periodic behavior but eventually becomes chaotic.

As r gets closer to r_c, the soluions still have a pattern that can be followed. However, once it passes beyond the critical value, r_c, the periodic behavior is no longer there, meaning there is no pattern to follow.

5.2 The Butterfly Pattern

Instead of plotting the solution we plot the trajectories for $y(t)$, on a phase plane of x(t) vs. z(t), we see what is known as the famous Butterfly Pattern. Figure 5.2 illustrates.

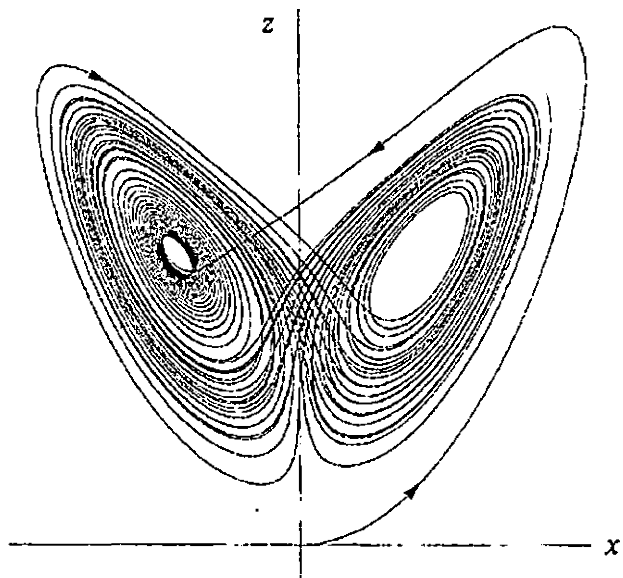

Figure 5.2: The Butterfly Pattern

Adapted from Chapter 1 of S.H. Strogatz. *Nonlinear Dynamics and Chaos: with applications to Physics, Biology, Chemistry, and Engineering.* Perseus Books Publishing, Cambridge, Maryland, 1994.

Through the Butterfly Pattern phase portrait it can also be seen that as time passes by, we cannot find periodic behavior. It is still very much aperiodic. As the tracjectory begins from the right hand side it then switches to the left. Once on the left it stays there, spiraling once or twice before going back to the right hand side. If we continue to follow the trajectory, there is no pattern of when it decides to move from left to right. It also seems that the trajectories are intersecting one another. However, this is not true if graphed in 3-dimensions! The trajectories do not intersect one another. Instead they either go in front or behind the other trajetories (see Figure 5.3).

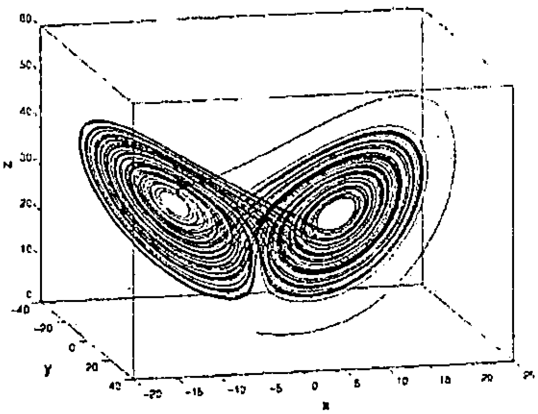

Figure 5.3: The Buttertly Pattern 3-Dimensions

Adapted from J. Sardanys. *Chaos.* http://complex.upf.es/~josep/Chaos.html, 2007.

Other than being called The Butterfuly Pattern, the image above is called a Lorenz attractor. The following image, will show 10,000 nearby conditions at times t = 3, 6, 9, and 15 [Str94]. The dark shade will show that as times goes by, even though they all started relatively at the same place and time, the end result could be anywhere on the strange attractor. Thus, long term behavior is chaotic. Predicting where it can land is not possible.

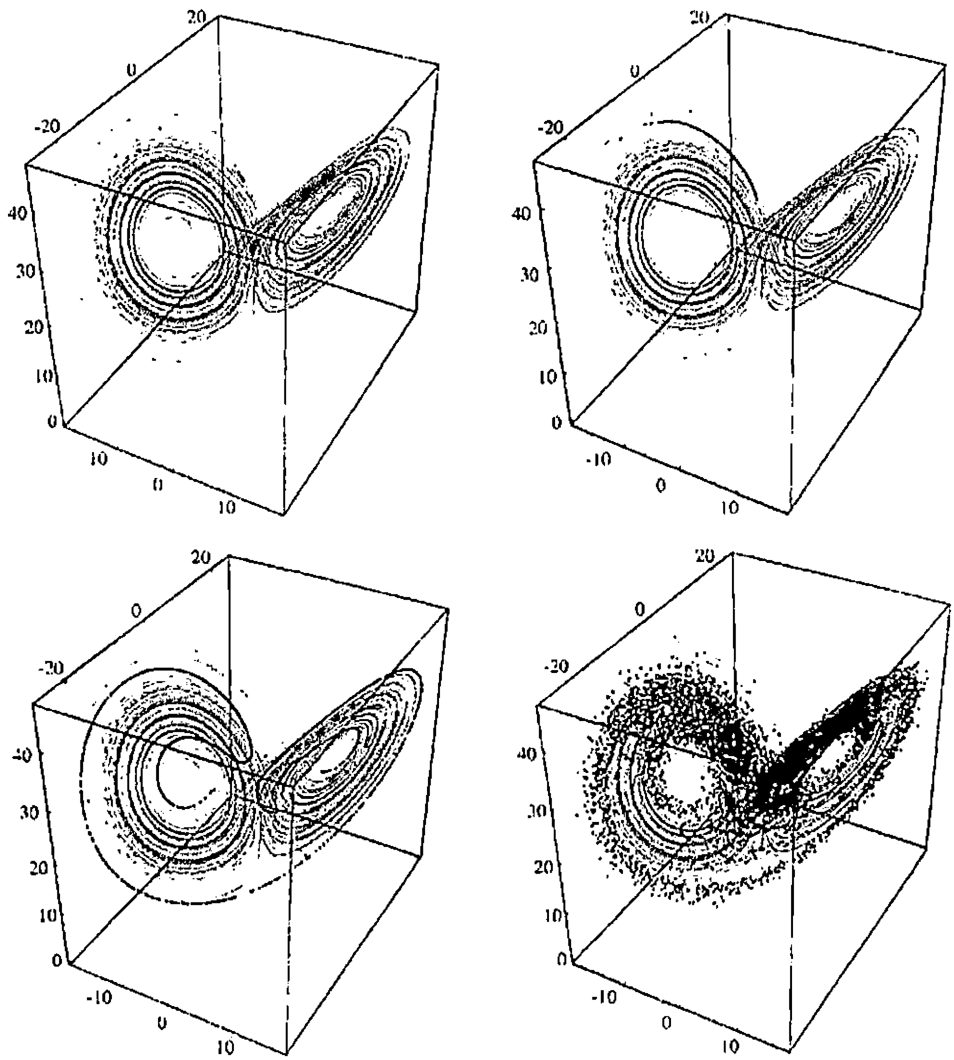

Figure 5.4: 10,000 Nearby Intitial Conditions at t = 3,6,9, and 15

Adapted from Chapter 8 of S.H. Strogatz. *Nonlinear Dynamics and Chaos: with applications to Physics, Biology, Chemistry, and Engineering.* Perseus Books Publishing, Cambridge, Maryland, 1994.

Appendix A: Homemade Waterwheel

While reading up on the Chaotic Waterwheel, I was curious to see this actual chaotic behavior. Thus, through the guidance of my father, Mariano Romero, and my friends, Santiago Mondragon Martinez and Armando Martinez, I built a waterwheel that replicated the same effects as the experiment that I mentioned above. Our waterwheel however does not look like the one made by Malkus and Howard, instead it was made from a bicycle wheel, a fish pump, and a 4-legged stand to lift the bicycle wheel; see the illustration below.

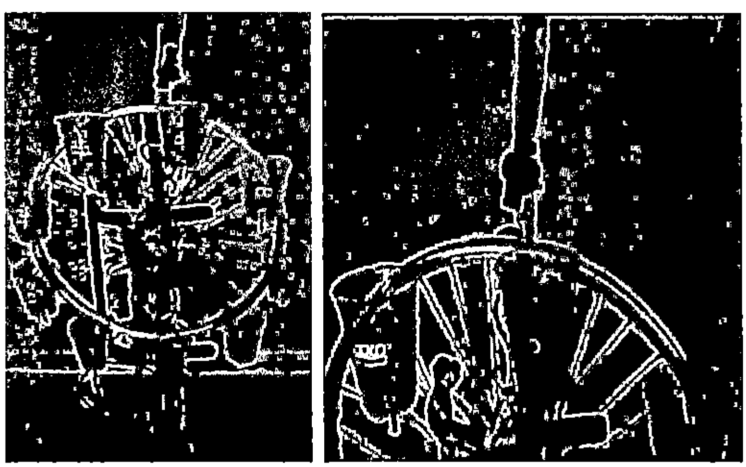

Figure A.1: Waterwheel and Nozzle

As you can see in the picture above, we numbered nine cups and attached them around the circumference of the bicycle wheel. Behind the wheel, we attached a plastic hose that will guide the water, being pumped by a fish pump, from the bottom to the top of the bicycle wheel. The idea of our experiment is that as the water, being affected by gravity, falls down vertically from the hose it will drop into the cups, forcing the bicycle wheel to turn to either the left or right direction. Now, each cup will have a hole on the bottom so the water can leak out and go back through the hose; a continuous water supply. Also, we attached a control valve at the top of the hose to control the inflow rate of the water.

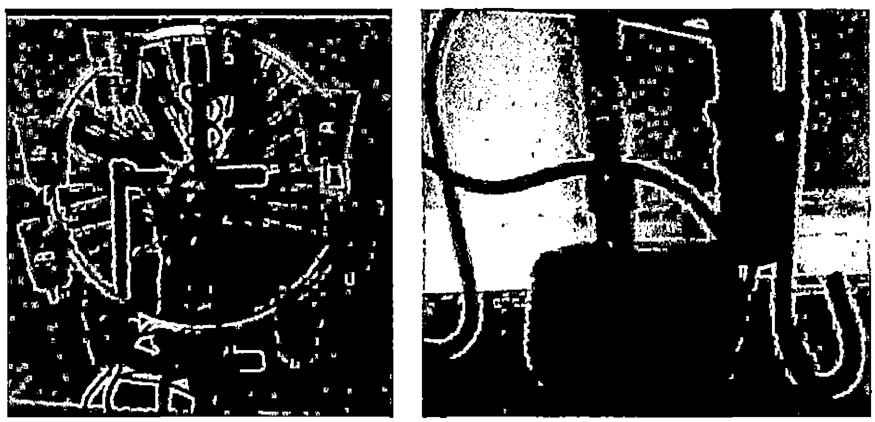

Figure A.2: Waterwheel and Fish Pump

Increasing the rate of water flow we started to notice periodic behavior. However, as time went by the experiment showed Chaotic behavior; for our waterwheel it took approximately two minutes. We were no longer able to find a pattern. When we thought there might be a pattern arising, sometimes the wheel stop and stay at rest. If the inflow rate of the water was changed, in this case decreased, then we were able to create a stable state in which the bicycle wheel rotated left or right in periodic behavior. Finally, decreasing the inflow rate even further created the state where the waterwheel was at rest.

Bibliography

[Cas05] B. Castello. *Dynamical Systems (550.391) Hopf Bifurcations.* `http://www.ams.jhu.edu/~castello/391/HopfBifurcations.pdf`, 2005.

[CJ09] A. Clark Jr. *ME 406 Bifurcations VII Subcritical Hopf Bifurcations.* `http://www.me.rochester.edu/courses/ME406/webexamp5/bifurc7.pdf`, 2009.

[Dra92] P. G. Drazin. *Nonlinear Systems.* Cambridge University Press, Cambridge, England, 1992.

[Lor63] E. N. Lorenz. Deterministic nonperiodic flow. *Journal of the Atmospheric Science*, 20:130–141, 1963.

[Sar07] J. Sardanys. *Chaos.* `http://complex.upf.es/~josep/Chaos.html`, 2007.

[Str94] S. H. Strogatz. *Nonlinear Dynamics and Chaos with applications to Physics, Biology, Chemistry, and Engineering.* Perseus Books Publishing, Cambridge, Maryland, 1994.